International Journal of Computer Applications in Engineering Sciences
[VOL I, ISSUE II, JUNE 2011] [ISSN: 2231-4946]

Hydrodynamic Modelling and CFD Simulation of Gas-Solid Bubbling Fluidized Bed

[1]Aditya Kashyap, [2]V.K Agarwal

Department of Chemical Engineering, Indian Institute of Technology Roorkee, Roorkee, India

[1] adiksh85@gmail.com
[2] vijayfch@iitr.ernet.in

Abstract— **This work presents a computational study of flow behaviour in a bubbling fluidized bed. The model is developed by using the commercial CFD code Fluent 6.3. The model is based on an Eulerian description of the gas and the particle phase. Different drag models are used and compared. The computational results are validated against experimental results. The experimental data are taken from Hulme (2005). This paper examines the effect of certain model parameters on bubble formation and bubble frequency. The dimension of the lab-scale fluidized bed is 0.1 × 0.1 × 1.00 m. The simulations are performed with spherical particles with mean particle size of 200 μm and density 2480 kg/m^3. The superficial gas velocity is 0.186 m/s. Computational results are compared mutually, as well as against experimental data.**

Keywords— **Multiphase flow; Fluidization; Computation; Modeling; CFD; Two-dimensional**

I. INTRODUCTION

Fluidised Bed Reactors are found in many operations in the chemical, petroleum, pharmaceutical, agricultural, biochemical, food, electronic, and power-generation industries. Fluidized beds are applied in industry due to their large contact area between phases, which enhances chemical reactions, heat transfer and mass transfer. The efficiency of fluidized beds is highly dependent of flow behaviour and knowledge about flow behaviour is essentially for scaling, design and optimization; however, the precise analysis of the flow field has not been achieved yet because of these complex phenomena between the gas and particles. In order to improve the performance of these processes of actual systems, detailed knowledge about the distribution of the different solid species throughout the bed in different operations is required. The mechanism for bubble formation, bubble growth and particle segregations are one of the most difficult research subjects in the gas bubbling fluidized beds Computational fluid dynamics, CFD is an emerging technique for predicting the flow behavior of these systems, as it is necessary for scale-up, design, or optimization [1].

In the last decade considerable progress has been made in the area of hydrodynamic modelling of the fluidized beds. Currently there are two approaches for the numerical calculation of multiphase flows: the Eulerian–Lagrangian approach and the Eulerian–Eulerian approach (TFM). In the Eulerian–Lagrangian approach, the fluid phase is treated as a continuum by solving the time averaged Navier–Stokes equations, while the dispersed phase is solved by tracking a large number of particles (or bubbles, droplets) through the calculated flow field. The dispersed phase can exchange momentum, mass, and energy with the fluid phase. A fundamental assumption made in this approach is that the dispersed second phase occupies a low volume fraction. In the Eulerian–Eulerian approach, the different phases are treated mathematically as interpenetrating continua. Since the volume of a phase cannot be occupied by the other phases, the concept of phase volume fraction is introduced. These volume fractions are assumed to be continuous functions of space and time and their sum is equal to one. For granular flows, such as flows in risers, fluidized beds and other suspension systems, the Eulerian –Eulerian multiphase model is generally used, and also for simulations in this study [11].Kinetic Theory of Granular flow is coupled with Eulerian model to describe the hydrodynamics of fluidised bed reactor.

Despite the modeling challenges, application of CFD to model fluidized bed hydrodynamics continues to develop, as it has many advantages including design optimization and scale-up of such systems. Some of the correlations used in the models, however, remain to be empirical or semi empirical. As a result, the model and its parameters must be validated against experimental measurements obtained at similar scale and configurations. In the present study the Eulerian approach is used to investigate gas-solid flow in a two dimensional fluidized bed. Gidaspow drag model and the drag model of Syamlal & O Brien are the default drag models in Fluent 6.3, and the simulations in the present study are based on these two drag models. The bubble behavior and bed properties are analyzed based on these two models.

II. PHYSICAL DESCRIPTION OF BED DYNAMICS

Computational studies have been performed on a 2-dimensional fluidized bed. Spherical particles with a

mean diameter of 200 μm and a density of 2480 kg/m^3 are used. The behaviour of particles in fluidized beds depends on a combination of their mean particle size and density. Geldart fluidization diagram [12], shown in Figure 1, is used to identify characteristics associated with fluidization of powders. The current particles are classified as Geldart B particles, but are very close to Geldart A particles. The fluidization properties for these two groups of particles differ significantly from each other.

Particles characterized in group A are easily fluidized and the bed expands considerably before bubbles appear. This is due to inter-particle forces that are present in group A powders [13]. Inter-particle forces are due to particle wetness, electrostatic charges and van der Waals forces. Bubble formation will occur when the gas velocity exceeds the minimum bubble velocity and the bubbles rise faster than the gas percolating through the emulsion. For group B particles the inter-particle forces are negligible and bubbles are formed as the gas velocity reaches the minimum fluidization velocity. The bubble size increases with distance above the gas distributor and increases also with increasing excess gas. The bed expansion is small compared to group A particles.

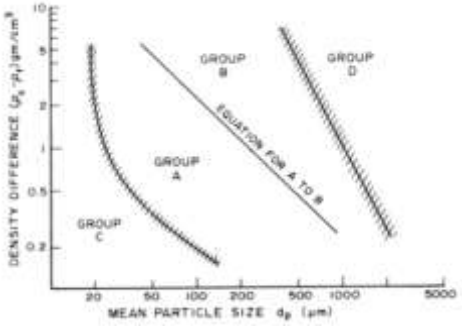

Fig. 1 Geldart classification of particles according to their fluidization behaviour [12]

III. Model Equations

The simulation of fluidized bed was performed by solving the governing equations of mass, momentum and energy conservation using Fluent 6.0 CFD software. A multi-fluid Eulerian model, which considers the conservation of mass and momentum for the gas and fluid phases, was applied. The kinetic theory of granular flow, which considers the conservation of solid fluctuation energy, was used for closure of the solids stress terms. The governing equations can be summarized as follows:

Conservation of Mass

$$\frac{\partial}{\partial t}(\alpha_g \rho_g) + \nabla(\alpha_g \rho_g \vec{v}_g) = 0 \quad (1)$$

$$\frac{\partial}{\partial t}(\alpha_s \rho_s) + \nabla(\alpha_s \rho_s \vec{v}_s) = 0 \quad (2)$$

Conservation of Momentum

$$\frac{\partial}{\partial t}(\alpha_g \rho_g \vec{v}_g) + \nabla(\alpha_g \rho_g \vec{v}_g^{\,2}) = -\alpha_g . \nabla P + \nabla . \bar{\bar{\tau}}_g + \alpha_g \rho_g \vec{g} + K_{gs}(\vec{v}_g - \vec{v}_s) \quad (3)$$

Phase Stress-Strain Tensor

$$\bar{\bar{\tau}}_g = \mu_g(\nabla \vec{v}_g + \nabla \vec{v}_g^{\,T}) + \left(\lambda_g - \frac{2}{3}\mu_g\right)\nabla \vec{v}_g \bar{\bar{I}} \quad (4)$$

$$\alpha_s \bar{\bar{\tau}} = -P_s \bar{\bar{I}} + \alpha_s \mu_s (\nabla \vec{v}_s + \nabla \vec{v}_s^{\,T}) + \left(\lambda_s - \frac{2}{3}\mu_s\right)\nabla \vec{v}_s \bar{\bar{I}} \quad (5)$$

TABLE 1

MOMENTUM EXCHANGE COEFFICIENTS

Interphase momentum exchange coefficient (drag models)

$$f_{drag} = K_{gs}(\vec{v}_g - \vec{v}_s)$$

Gidaspow (1986) model

$$K_{gs}^{Ergun} = 150\frac{\alpha_s^2 \mu_g}{\alpha_g d_s^2} + 1.75\frac{\alpha_s \rho_g}{d_s}|\vec{v}_s - \vec{v}_g|, \ \alpha_g < 0.8$$

$$K_{gs}^{Wen-Yu} = \frac{3}{4}C_D \frac{\alpha_s \alpha_g \rho_g}{d_s}|\vec{v}_s - \vec{v}_g|\alpha_g^{-2.65}, \ \alpha_g \geq 0.8$$

where

$$C_D = \begin{cases} \frac{24}{\alpha_g \mathrm{Re}_s}[1 + 0.15(\alpha_g \mathrm{Re}_s)^{0.687}], & \mathrm{Re}_s < 1000 \\ 0.44 & \mathrm{Re}_s \geq 1000 \end{cases}$$

$$\mathrm{Re}_s = \frac{\rho_s d_s |\vec{v}_s - \vec{v}_g|}{\mu_g}$$

Syamlal and O'Brien (1988) model

$$K_{gs} = \frac{3}{4}\frac{C_p}{v_{r,s}^2}\frac{\rho_g |\vec{v}_s - \vec{v}_g|}{d_s}\alpha_g \alpha_s$$

$$C_D = \left(0.63 + \frac{4.8}{\sqrt{(\mathrm{Re}_s / v_{r,s})}}\right)^2$$

$$\mathrm{Re}_s = \frac{\rho_g d_s |\vec{v}_s - \vec{v}_g|}{\mu_g}$$

$$v_{r,s} = 0.5(A - 0.06\mathrm{Re}_s + \sqrt{(0.06\mathrm{Re}_s)^2 + 0.12\mathrm{Re}_s(2B - A) + A^2})$$

with

$$A = \alpha_g^{4.14}; \ B = \begin{cases} \alpha_g^{C_1} & \alpha_g \geq 0.85 \\ C_2 \alpha_g^{1.28} & \alpha_g < 0.85 \\ C_1 = 2.65 \text{ and } C_2 = 0.8 \end{cases}$$

TABLE 2

CONSTITUTIVE EQUATIONS

Solid Pressure

$$P_s = 2\rho_s (1+e_{ss}) \alpha_s^2 g_{0,ss} \theta_s$$

Radial Distribution Function

$$g_{0,ss} = \left[1-\left(\frac{\alpha_s}{\alpha_{s,\max}}\right)^{1/3}\right]^{-1}$$

Bulk Viscosity

$$\lambda_S = \frac{4}{3}\alpha_S \rho_S d_S g_{0,ss} (1+e_{ss}) \left(\frac{\theta_s}{\pi}\right)^{1/2}$$

Solid shear stress

$$\mu_s = \mu_{s,col} + \mu_{s,kin} + \mu_{s,fr}$$

Collisional viscosity

$$\mu_{s,col} = \frac{4}{5}\alpha_s \rho_s d_s g_{0,ss}(1+e_{ss}) \left(\frac{\theta_s}{\pi}\right)^{1/2}$$

Kinetic viscosity

$$\mu_{s,kin} = \frac{\alpha_s d_s \rho_s \sqrt{\theta_s \pi}}{6(3-e_{ss})}\left[1+\frac{2}{5}(1+e_{ss})(3e_{ss}-1)\alpha_s g_{0,ss}\right]$$

Frictional viscosity

$$\tau_{friction} = -P_{friction}\,\vec{\vec{I}} + \mu_{friction}(\nabla\vec{u}_s + (\nabla\vec{u}_s)^T)$$

$$P_s = P_{kinetic} + P_{friction}$$

$$\mu_s = \mu_{kinetic} + \mu_{friction}$$

Frictional pressure (Johnson and Jackson, 1987)

$$P_{friction} = Fr\,\frac{(\alpha_s - \alpha_{s,\min})^2}{(\alpha_s - \alpha_{s,\max})^3}$$

$$\mu_{friction} = P_{friction}\sin\phi$$

$$Fr = 0.1\,\alpha_s$$

Granular temperature

$$\frac{3}{2}\left[\frac{\partial}{\partial t}(\rho_s\alpha_s\theta_s) + \nabla(\rho_s\alpha_s\vec{v}_s\theta_s)\right] = (-p_s\vec{\vec{I}} + \vec{\vec{\tau}}_s):\nabla v_s + \nabla(k_{\theta s}\nabla\theta_s) - \gamma_{\theta s} + \phi_{gs}$$

Diffusion coefficient for granular temperature

$$k_{\theta s} = \frac{15 d_s \rho_s \sqrt{\theta_s \pi}}{4(41-33\eta)}\left[1+\frac{12}{5}\eta^2(4\eta-3)\alpha_s g_{0,ss} + \frac{16}{15\pi}(41-33\eta)\eta\alpha_s g_{0,ss}\right]$$

$$\eta = \frac{1}{2}(1+e_{ss})$$

Collisional dissipation energy

$$\gamma_{\theta s} = \frac{12(1-e_{ss}^2)\, g_{0,ss}}{d_s\sqrt{\pi}}\,\rho_s\,\alpha_s^2\theta_s^{3/2}$$

Transfer of kinetic energy between phases

$$\phi_{gs} = -3K_{gs}\theta_s$$

IV. COMPUTATIONAL SET-UP

A computational study of bubble behaviour in a 3-D fluidized bed is performed. The cross section area of the bed is 0.1 m × 0.1 m and the height is 1.0 m. The initial particle height is 0.4 m, and the initial void fraction in the packed bed is 0.55. A three dimensional Cartesian co-ordinate system is used to describe the fluidized bed. The grid resolution is 10 mm in horizontal and vertical direction and the total number of control volumes is 125000. Spherical particles with a diameter of 200 μm and density 2480 kg/m^3 are used. The coefficient of restitution is set to 0.9. The boundary conditions are given as velocity inlet and pressure outlet. The inlet superficial gas velocity is set to 0.186 m/s and the outlet pressure is 1 atm. The simulations are run for about 3 s real time, and the computational results are compared to experimental data obtained on a corresponding fluidized bed with the same set-up and flow conditions. The calculated minimum fluidization velocity for particles with diameter of 200 μm and density 2480 kg/m^3 is 0.093 m/s [6], and according to Geldart fluidization diagram the particles are characterized as B particles.

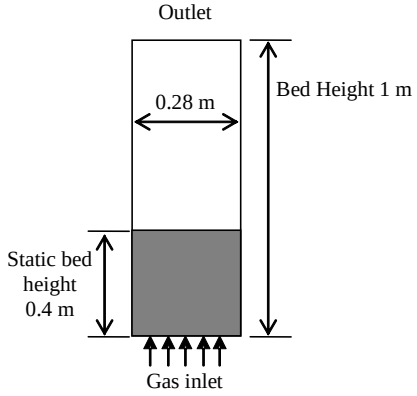

Fig. 2 Schematic representation of 2-D fluidized bed reactor

TABLE 3

SIMULATION MODEL PARAMETERS

Description	Value	Comment
Particle density, ρ_p	2480 kg/m^3	Glass beads
Gas density, ρ_g	1.225 kg/m^3	Air
Mean particle diameter, d_p	200 μm	Uniform distribution
Restitution coefficient, ε_{ss}	0.9/0.99	Range in literature
Initial solids packing, ε_{s0}	0.60	Fixed value
Superficial gas velocity, U	0.025-0.51 ms	~0.5-~6 U_{mf}
Bed width	0.28 m	Fixed value
Bed height	1 m	Fixed value
Static bed height	0.40 m	Fixed value
Grid interval spacing	0.005 m	Specified
Inlet boundary conditions	Velocity	Superficial gas velocity
Outlet boundary conditions	Outflow	Fully developed flow
Time steps	0.001 s	Specified
Maximum number of iterations	20	Specified
Convergence criteria	10^{-3}	Specified

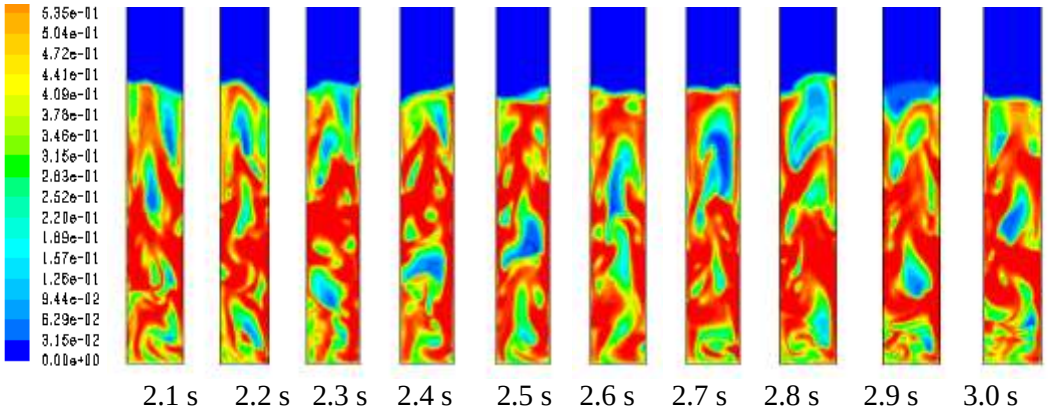

Fig. 3 Contours of Volume Fraction of Solids for Gidaspow drag model

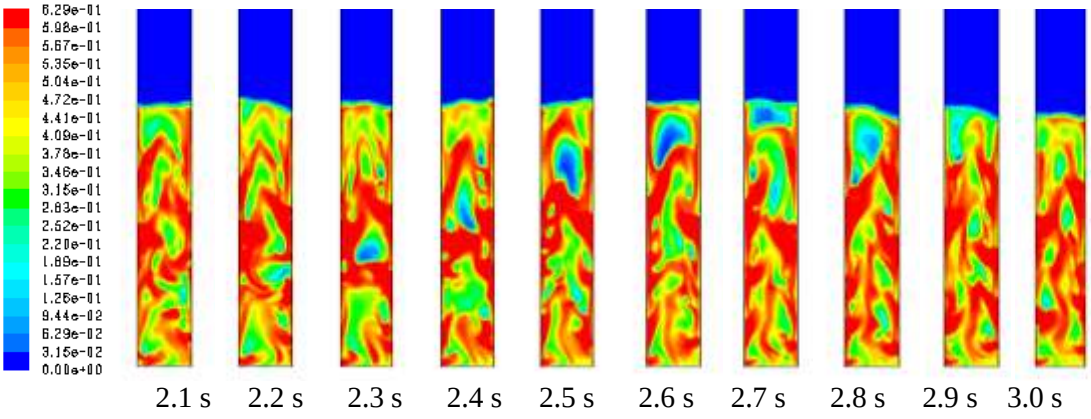

Fig. 4. Contours of Volume Fraction of Solids for Gidaspow drag model

V. Results and Discussion

The simulations are run with Syamlal & O Brien drag model and with Gidaspow drag model. Figure 5 shows the mean void fraction as a function of radial position in the bed. The results are presented at height 0.1 m and 0.35 m. The results from the two drag models give no significant difference in void fraction.

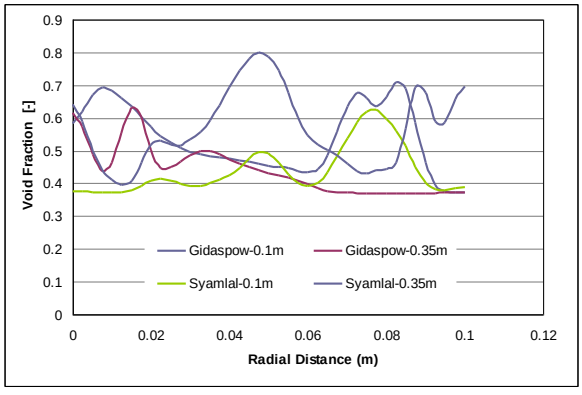

Fig. 5 Void fractions as a function of radial position at different bed heights.

Both models give low void fraction in the centre of the bed, and that indicates that the bubble frequency is low in this area. The Bed height, bed voidages, and mean densities are related as;

$$\frac{L_f}{L_{mf}} = \frac{1-\varepsilon_{mf}}{1-\varepsilon_f} \tag{30}$$

The void fraction in the packed bed is 0.45, and according to the results shown in Figure 1, the mean void fraction in the fluidized bed is about 0.54. That means that the bed has expanded significantly, from initial bed height 0.4 m to a bed height of about 0.49 m. The mean bed height in the experimental fluidized bed was 0.42 m. The over prediction of the bed height from these two drag models can also be understood from the contours of volume fraction of solid as shown in Fig.3 and 4.However, a more extensive grid study may yield a decreased average bed height.

Another important quantity is the pressure drop across the bed. The pressure drop for the bed can be calculated using the following equation.

$$\frac{\Delta P}{L} = \varepsilon_{mf}\,(\rho_s - \rho_g)\,g \tag{31}$$

The calculated pressure drop is approximately 5300 Pa compared to the simulated pressure drop of 5350 Pa. Both these values are within 3% of the average experimental pressure drop of 5150 Pa.

In this study the computational bubbles are defined as void fractions higher than 0.6. A gas bubble has low solid density, sometimes called gas pockets or voids, however it has been observed from the experimental study that parts of the bubbles can include high fractions of solids. Another reason for using a rather low void fraction in the definition of bubbles is that bubbles might occupy only a part of the control volume, and the mean void fraction for the control volume will then be lower than the void fraction in a bubble but higher than the mean void fraction in the bed. Figure 6(a) and (b) shows a plot of void fraction as a function of time at one position in the bed for Gidaspow and Syamlal Drag Model. The plot shows the bubble frequency for different drag models. Bubble frequency is a probe which records the frequency of bubbles passing a given point in the bed. It can be seen that the void fraction in this point varies from 0.48 to 0.62. The highest peaks represent the bubbles. Bubble frequency is a probe which records the frequency of bubbles passing a given point in the bed. It can be seen that the void fraction in this point varies from 0.48 to 0.62. The highest peaks represent the bubbles.

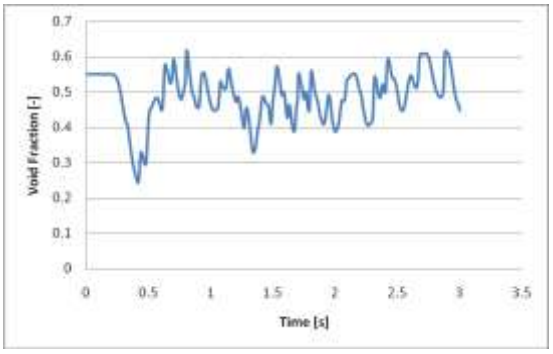

Fig. 6(a) Bubble frequency as a function of time for Gidaspow Drag Model at No-Slip Condition

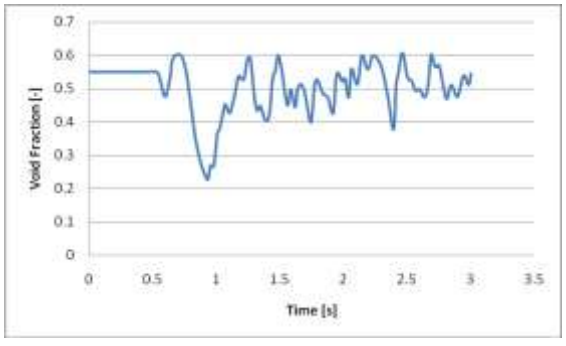

Fig. 6(b) Bubble frequency as a function of time for Syamlal Drag Model at No-Slip Condition

Figure 7 shows the bubble frequency when partial-slip boundary condition is applied to the walls with specularity coefficient of 0.5. It can be seen that the occurrence of bubbles is more frequent when we apply the partial slip conditions to the walls.

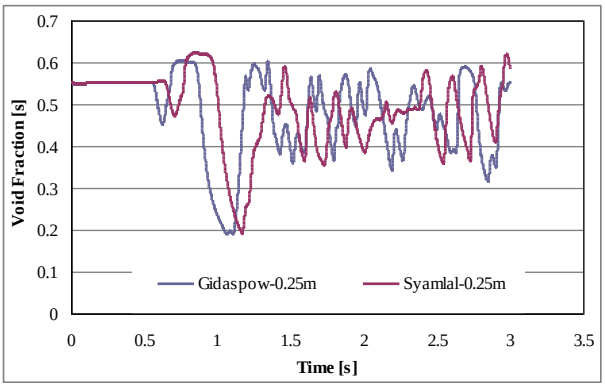

Fig. 7 Bubble frequency as a function of time for Syamlal Drag Model at No-Slip Condition

Fig. 8 shows the velocity vectors of glass beads in the column obtained at inlet air velocity of 0.186 m/s for static bed height 0.4 m and glass beads of size 200µm after the quasi steady state has been achieved. The velocity vectors are helpful in determining flow patterns in fluidized bed. In the upper part of the fluidizing section there is a circulatory motion of the particles, near the wall direction of velocity is downward while that in the central zone the direction is upward. The velocity vector of solid phase in the column is mostly upward, but in the fluidized section the magnitude is more and little back mixing of the liquid is also seen in this section. The solids are carried by the gas upwards by the bubbles, move up in the reactor and the as the bubble coalesce the solids drops to the bottom again. This circulatory motion and rigorous interaction between the solid and gas phase results in high heat and mass transfer and better mixing.

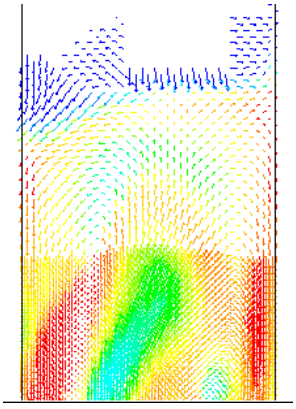

Fig. 8 Velocity Vectors of Solid

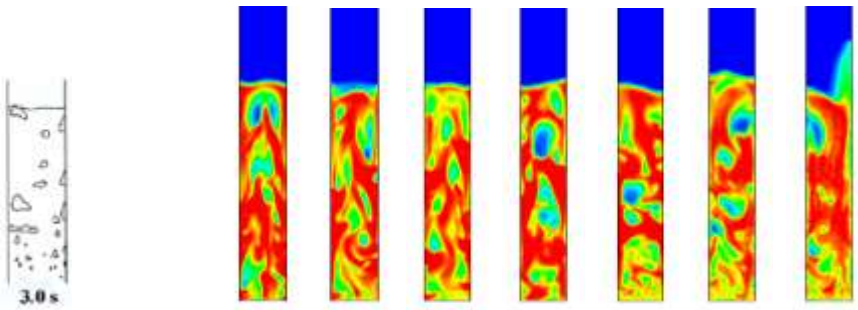

Laux & Johnson (1988) e = 0.73 e = 0.80 e = 0.90 e = 0.95 e = 0.97 e = 0.99 e = 1.00

Fig. 9 Contours of solid volume fraction at different coefficient of restitution

Fig. 9 shows snapshots of the experiment carried out by Laux and Johnson (1988) and contours of volume fraction of solid for various values of the coefficient of restitution at the moment of bubble eruption at the bed surface. It can be seen that as collisions become less ideal (and more energy is dissipated due to inelastic collisions) particles become closely packed in the densest regions of the bed, resulting in sharper porosity contours and larger bubbles. From the figure it is clear that that the simulation with e = 0.97 does not show the best resemblance with the experiment.

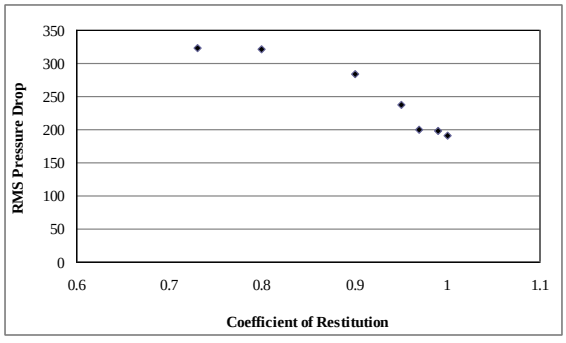

Fig. 10

Fig.2 shows the root mean square (RMS) of the pressure fluctuations is presented as a function of the coefficient of restitution (the initial 2 s of the simulations were not taken into account). From the figure, it can be seen that the intensity of pressure fluctuations in the bed decreases gradually when the coefficient of restitution approaches 1.

VI. Discussion

The low bubble frequencies in the simulations can be explained by the difference in the calculated and the experimental minimum fluidization velocity. The theoretical minimum fluidization velocity for spherical particles is given by:

$$U_{mf} = \frac{d_p^2 \, \Delta\rho . g}{\mu} . \frac{\alpha_{mf}^3}{1-\alpha_{mf}} \qquad (32)$$

where, $\frac{\alpha_{mf}^3}{1-\alpha_{mf}}$ is approximately 11 [8].

The theoretical minimum fluidization velocity for the current particles is 0.0012 m/s, whereas in the experimental study, the observed minimum fluidization velocity was 0.093 m/s. In the experimental study, glass particles with a mean diameter of 200 μm were used. These particles have a particle size distribution that will influence on the flow conditions in the bed. This is not accounted for in the simulations. To account for the particle size distribution, the simulations can be run with multiple particle phases with different diameters. The particle size distribution in the experimental fluidized bed influences on the minimum fluidization velocity, and it was also observed that the particles behaved more like Geldart A particles, where the bed expands considerably before the bubbles appear. For group A particles bubbles appear as the gas velocity exceeds the minimum fluidization velocity, whereas for group B particles bubbles appear as the gas velocity reaches the minimum fluidization velocity.

The excess gas velocity is defined as the difference between the superficial gas velocity and the minimum fluidization velocity. In the experiments, the ratio between the superficial gas velocity and the minimum fluidization velocity was about 2 whereas in the simulations this ratio is about 7. The high excess gas velocity, results in high bed expansion and thereby high mean void fraction in the bed. The conditions for bubble formations are then changed, and well defined bubbles may not appear.

VII. Conclusion

The CFD code Fluent 6.3 is used to study flow behaviour in a 3-dimensional bubbling fluidized bed. The Eulerian approach is used to describe the gas and the solid phase. The simulations are performed with Gidaspow drag model and the drag model developed by Syamlal & O Brian. The results from the simulations with these two drag models do not differ significantly from each other. Both the models give high bed

expansion, and a rather low bubble frequency. The bed expands from 0.75 m to about 1.0 m, and the bubble frequencies are about 0.5 s^{-1}. Well defined bubbles, that means a region of void fraction greater than 0.80, are only observed in the first 4 seconds. The Syamlal & O Brian drag model gives slightly higher bubble frequency than the Gidaspow drag model.

The simulations are compared to experimental results. The experimental study is performed with spherical glass particles with mean particle size of 154 μm and density 2485 kg/m^3. The initial particle height is 0.75 m and the superficial gas velocity is 0.133 m/s. The same conditions are used for the simulations. In the experiments, however, the particles have a size distribution that covers particle sizes from about 50 m to 250 m. In the simulation all the particles are defined with the same diameter, 154 μm. The simulations give considerably lower bubble frequencies than the experiments. The experimental bubble frequency is about 2 s^{-1}, and that is about 4 times the bubble frequencies obtained in the simulations. The bed expansion in the experiments is about 0.1 m, whereas it is about 0.25 m in the simulations. The discrepancies between computational and experimental result may be due to the different ranges of particle sizes. The observed experimental minimum fluidization velocity is about 4 times the calculated minimum fluidization velocity for particles with diameter 154 μm. The consequence of this is that the excess gas velocity becomes much higher in the simulations than in the experiments, and the ideal conditions for a bubbling fluidized bed might no longer be present. To get a better agreement between simulations and experiments, the simulations should be performed with multiple particle phases to account for the particle size distribution in the experiments.

NOMENCLATURE

C_D	[-]	Friction coefficient
d_s	[m]	Particle diameter
e	[-]	Coefficient of restitution
g_i	[m/s^2]	Acceleration due to gravity
g_0		Radial distribution function
K_{qm}	[kg/m^3·s]	Coefficient for the interface force between the fluid phase and the solid phase
p	[Pa]	Fluid pressure
p_s	[Pa]	Solid phase pressure
Re_s	[-]	Particle Reynolds number
U_{qi}	[m/s]	Velocity vector for phase q
v_r	[m/s]	Terminal velocity
Special characters		
α_q	[-]	Volume fraction of phase q
ρ_q	[kg/m^3]	Density of phase q
$\bar{\tau}_{ij}$	[kg/m·s^2]	Stress tensor
μ	[kg/m·s]	Viscosity
ξ_s	[kg/m·s]	Bulk viscosity
Θ_s	[m^2/s^2]	Granular temperature
Subscripts		
i, j, k		i, j and k directions
g		Gas phase
s		Solid phase

REFERENCES

[1] L. Huilin, H. Yuronga, and D. Gidaspow, "Hydrodynamic modelling of binary mixture in a gas bubbling fluidized bed using the kinetic theory of granular flow," Chemical Engineering Science, 58, pp. 1197-1205, 2003.

[2] J.A.M. Kuipers and W.P.M. Van Swaaij, Adv. Chem. Eng. 24, pp. 227-328, 1998.

[3] M.J.V. Goldschmidt, B.P.B. Hoomans and J.A.M. Kuipers, "Recent progress towards hydrodynamic modeling of dense gas –particle flows," Recent Res. Dev. Chem. Eng. 4,, pp. 273-292, 2000.

[4] M.J.V. Goldschmidt, J.A.M. Kuipers and W.P.M. Van Swaaij, "Hydrodynamic modeling of dense gas-fluidised beds using the kinetic theory of granular flow: effect of the coefficient of restitution on bed dynamics," Chem. Eng. Sci. 56,, pp. 571-578, 2001.

[5] J.A. Yasuna, H.R. Moyer, S. Elliott, and J.L. Sinclair, "Quantitative predictions of gas-particle flow in vertical pipe with particle-particle interactions," Powder Technology 84, pp. 23-34, 1995.

[6] B. Halvorsen and V. Mathiesen, "CFD Modelling and simulation of a lab-scale Fluidised Bed," Modeling, Identification and Control, 23(2), pp. 117-133, 2002.

[7] C.H. Ibsen, An experimental and Computational Study of Gas-Particle Flow in Fuidised Reactors, Ph.D. Thesis, Aalborg University, Esbjerg, 2002.

[8] G.A. Bokkers, M. van Sint Annaland, and J.A.M. Kuipers, "Mixing and segregation in a bidiperse gas-solid fluidised bed: a numerical and experimental study," Powder Technology, 140, pp. 176-186, 2004.

[9] S. Ergun, "Fluid flow through packed columns," Chemical Engineering Progress 48(2), pp. 89-94, 1952.

[10] D. Gidaspow, Multiphase Flow and Fluidization. Academic Press, Boston, 1994.

[11] P.N. Rowe, "Drag forces in a hydraulic model of fluidized bed-Part II," Trans. Instn. Chem., 39, pp. 175-180, 1961.

[12] C.Y. Wen and Y.H. Yu, "Mechanics of Fluidization," Chemical Engineering Progress, 62, pp. 100-111, 1966.

[13] L.G. Gibilaro, R. Di Felice, and S.P. Waldram, "Generalized Friction Factor and Drag Coefficient for Fluid-Particle Interaction," Chemical Engineering Science 40(10), pp. 1817-1823, 1985.

[14] M. Syamlal and T.J. O Brien, "A generalized drag correlation for multiparticle systems," Morgantown Energy Technology Center, DOE Report, 1987.

[15] J.T. Jenkins and S.C. Cowin, "Theories for flowing granular materials, mech. applied to transport of bulk materials," Ap. Mech. Div. of ASME, 31, pp. 79-89, 1979.

[16] D. Geldart, "Types of Gas Fluidization," Powder Technology, 7, 1973, pp. 285-295.

[17] D. Geldart, Gas Fluidization Technology, John Wiley & Sons Ltd., 1986.

[18] Fluent, Fluent 6.2 Users Guide, Fluent Inc., Lebanon, NH, USA, 2005.

[19] R.A. Bagnold, "Experiments on a Gravity-Free Dispersion of Large Solid Spheres in a Newtonian Fluid Under Shear," Proc. of Roy. Soc., A225, pp. 49-63, 1954.

[20] B. Halvorsen, An Experimental and Computational Study of Flow Behaviour in Bubbling Fluidized Beds, Doctoral Thesis at NTNU: 70, 2005.